

# Performance and Complexity Trade-off Optimization of Speech Models During Training

Esteban Gómez, Tom Bäckström *Senior Member, IEEE*

**Abstract**—In speech machine learning, neural network models are typically designed by choosing an architecture with fixed layer sizes and structure. These models are then trained to maximize performance on metrics aligned with the task’s objective. While the overall architecture is usually guided by prior knowledge of the task, the sizes of individual layers are often chosen heuristically. However, this approach does not guarantee an optimal trade-off between performance and computational complexity; consequently, post hoc methods such as weight quantization or model pruning are typically employed to reduce computational cost. This occurs because stochastic gradient descent (SGD) methods can only optimize differentiable functions, while factors influencing computational complexity, such as layer sizes and floating-point operations per second (FLOP/s), are non-differentiable and require modifying the model structure during training. We propose a reparameterization technique based on feature noise injection that enables joint optimization of performance and computational complexity during training using SGD-based methods. Unlike traditional pruning methods, our approach allows the model size to be dynamically optimized for a target performance-complexity trade-off, without relying on heuristic criteria to select which weights or structures to remove. We demonstrate the effectiveness of our method through three case studies, including a synthetic example and two practical real-world applications: voice activity detection and audio anti-spoofing. The code related to our work is publicly available to encourage further research.

**Index Terms**—Speech machine learning, low-complexity, voice activity detection, deep fake detection.

## I. INTRODUCTION

NEURAL NETWORK models have achieved remarkable performance across numerous speech processing applications, often outperforming traditional digital signal processing methods. Consequently, they are often highlighted as state-of-the-art solutions in survey papers, offering superior results in tasks such as speech enhancement [1], audio anti-spoofing [2], or automatic speech recognition [3], among others. However, these networks typically require significantly more computational resources to model more complex functions than their predecessors. This results in higher minimum hardware requirements for running such solutions, and increased energy consumption across various devices.

Nevertheless, the connection between a model’s performance and its complexity (i.e., computational cost) is usually nonlinear. Although larger and more complex models are generally expected to show performance improvements,

The authors are with the Department of Information and Communications Engineering, Aalto University, Espoo, Finland (e-mail: esteban.gomez.mellado@aalto.fi; tom.backstrom@aalto.fi).

Manuscript received April 19, 2021; revised August 16, 2021.

these improvements are often not directly proportional to the increase in complexity. Instead, they frequently exhibit diminishing marginal returns, in which significant increases in complexity yield only modest performance gains.

As an example, the study by Braun et al. on noise suppression [4] shows that doubling the complexity of the NSNet2-R model from 2 MMACs to 4 MMACs, where MACs refer to multiply-accumulate operations - a common measure of computational complexity - results in an improvement in  $\Delta$ MOS - the difference in Mean Opinion Score - of approximately 0.05. However, further increasing complexity from 4 MMACs to 8 MMACs yields a smaller  $\Delta$ MOS improvement, with performance saturation observed beyond 6 MMACs.

Similarly, Yakovlev et al. demonstrated that their speaker recognition network achieved an absolute improvement in Equal Error Rate (EER) of approximately 0.2 %, decreasing from 1.2 % to 1.0 %, when the complexity was doubled from ReDimNet-B1 (approximately 0.5 GMACs) to ReDimNet-B2 (approximately 1 GMACs) [5]. However, further reducing the EER from 1.0 % to 0.8 % required an additional increase in complexity to approximately 5 GMACs from ReDimNet-B2 to ReDimNet-B4.

Although training objectives typically aim to maximize performance for a given task without necessarily considering complexity, significantly larger models that offer only modest or marginal gains in performance may be neither advantageous in practical scenarios nor energy-efficient [6]. In contrast, maintaining a lower computational budget provides several benefits, such as enabling faster inferences, facilitating on-device deployment on constrained hardware, and reducing the energy footprint, which can also extend the lifespan of battery-driven devices.

A key challenge in directly including a complexity related term as part of the training objective, is that factors related to the complexity of a model are expressed through non-differentiable discrete values, such as layer sizes or floating-point operations per second (FLOP/s), which are incompatible with gradient descent-based optimization methods. Additionally, layer sizes are typically fixed once the model is instantiated, so adjusting complexity during training would require modifying the layer sizes dynamically. Due to these constraints, various alternatives have been proposed to optimize the performance and complexity trade-off.

During training, techniques such as dropout [7] and regularization [8] improve performance by preventing overfitting and minimizing reliance on specific weights, without adding computational cost during inference. However, these methods

do not change the model’s architecture, limiting their ability to remove redundant layers.

Quantization-aware training (QAT) [9] reduces complexity by using lower-precision numeric types, such as int8, aiming to minimize inaccuracies from converting floating-point arithmetic to these lower-precision formats. Yet, to be effective, this approach requires specific hardware features, and does not modify the original architecture [10].

Knowledge distillation [11] transfers the capabilities of a larger “teacher” model to a smaller “student” model, effectively changing the resulting architecture. However, it requires careful selection of models tailored to the specific task [12].

Model pruning [13] features both training and post-training variants, with structured and unstructured approaches. Unstructured pruning removes less important weights, resulting in sparse tensors, but requires high degrees of sparsity for a substantial complexity reduction [14]. Structured pruning reduces complexity by systematically removing entire channels, or layers. However, it often relies on heuristics or empirical observations and requires a tailored iterative process for specific architectures and tasks.

Additional post-training methods, such as layer fusion [15], can optimize the computational graph to improve efficiency, but they do not modify the architecture itself (i.e., layer sizes).

To address these limitations, we present a novel differentiable method based on feature noise injection and dynamic complexity layers, as detailed in Section III. Our approach reduces manual decision-making and balances performance and complexity during training, resulting in models with smaller layer sizes and lower overall complexity. In Sec. IV to VI, we apply the proposed method on simulated data, voice activity detection (VAD), and audio anti-spoofing, respectively. We show that this method alone can significantly decrease computational complexity by more than 80 % in models with significant redundancy, while simultaneously reducing the size by approximately 90 %. Moreover, our method can be combined with the techniques above to compress the model further. We provide open access to the code for our method to encourage further research<sup>1</sup>.

## II. RELATED WORK

Neural networks, ubiquitous in speech machine learning, pose challenges due to their high computational and energy demands, leading to increased operational costs and usage limitations in real-world scenarios. For this reason, researchers have pursued various strategies to reduce the complexity of training and inference. Central to these efforts is the “Lottery Ticket Hypothesis” [16] of Frankle et al., which proposes that within large networks, smaller subnetworks (“winning tickets”) can independently achieve similar performance with fewer parameters and lower computational cost, highlighting the issue of overparameterization.

In the following subsections, we detail existing efforts to reduce complexity, and then introduce our novel approach based on feature noise injection and dynamic complexity layers, which we further explain in Section III. We focus

the discussion on methods that address model complexity directly, excluding hardware optimizations and approaches that enhance computational efficiency without modifying the model architecture.

### A. Model pruning

Model pruning was first introduced by LeCun et al. in their seminal work, “Optimal Brain Damage” [17], and has since been further studied and extended by numerous researchers [18]–[22]. It consists of removing unnecessary parameters from a network to reduce its complexity.

Pruning can be implemented during training or as a post-training procedure, and requires selecting a criterion such as weight magnitude or gradient-based analysis, resulting in either structured or unstructured pruning. While unstructured pruning primarily enhances sparsity by eliminating individual weights, structured pruning can remove entire components, such as channels or layers, producing a simpler model that maintains performance. However, model pruning often introduces additional difficulty to the training procedure and may require further fine-tuning after the weights are effectively removed. Additionally, common criteria, such as weight magnitude, may not consistently reflect the importance of parameters across different tasks.

### B. Knowledge distillation

This method first selects a teacher model that performs well on a particular task. The teacher’s outputs are then used to guide the training of a smaller student model, akin to selecting the “winning ticket” of the Lottery Ticket Hypothesis in advance, thereby preserving essential predictive capabilities while reducing complexity. Although this approach has been successfully applied to speech machine learning tasks [23]–[26], it faces challenges, including reliance on the quality of the teacher model, increased training difficulty, and potential information loss during distillation. Additionally, biases and errors in the teacher model may be transferred to the student, potentially affecting its performance and generalization.

### C. Neural architecture search (NAS)

The goal of this method is to automatically design neural networks by navigating a predefined search space of potential architectures. This approach involves defining an appropriate search space and applying strategies such as evolutionary algorithms, Bayesian optimization, or reinforcement learning to discover optimal network configurations [27]. NAS has been successfully applied to various speech processing tasks, including text-to-speech [28], automatic speech recognition [29], and speech separation [30].

However, NAS can be computationally intensive and often requires numerous trials to explore a vast search space effectively. This requires significant computational resources, which can limit accessibility and reproducibility [31]. Furthermore, the success of NAS is highly dependent on the design of evaluation procedures, which – if not carefully implemented – can result in models that are suboptimal or overfit to specific datasets and fail to generalize well.

<sup>1</sup>[URL will be provided upon publication]

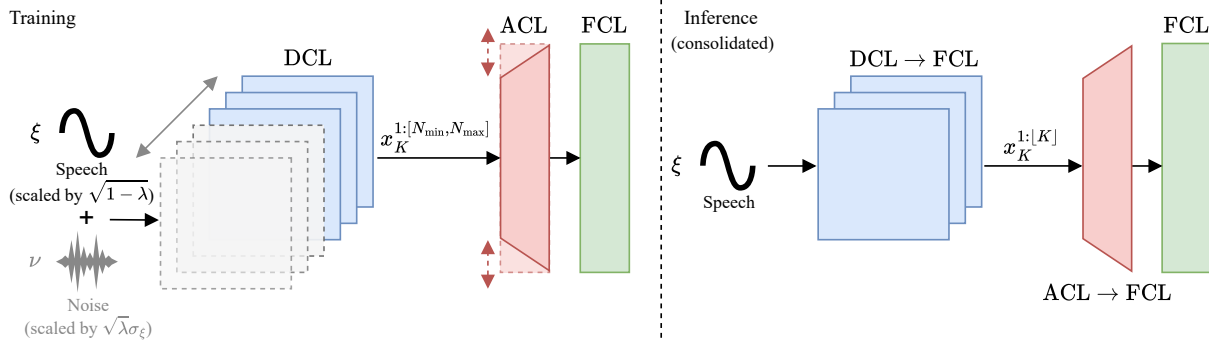


Fig. 1. Dynamic (DCL), adaptive (ACL) and fixed (FCL) complexity layers. During training, DCL can modify their output shape, whereas ACL will adapt their input shape to remain compatible, and FCL have fixed shape during training. At inference time, all layers are consolidated to their final fixed shape.

#### D. Dynamic neural networks

Dynamic neural networks (DynNN) adjust their architecture during inference based on input characteristics, scaling computational resources according to input difficulty [32]. This efficient resource allocation allocates more computational resources to challenging inputs and less to simpler ones. However, this method requires design strategies capable of operating across varying levels of network utilization, such as early exit [33] or slimming [34], which may be specific to each architecture. Additionally, inference speed is nondeterministic and fluctuates with each particular input.

#### E. Proposed method

In contrast to the aforementioned methods, our approach involves injecting uncorrelated noise into model features to automatically assess their importance. We hypothesize that weights capable of tolerating high levels of noise without degrading performance are less critical to the model, and can potentially be removed, whereas weights sensitive to noise are essential and should be retained. Unlike NAS, our method is differentiable and applicable during training within a single trial, operates independently of the architecture, and, unlike DynNN, results in permanent model complexity reduction. Our technique can be viewed as a form of structured pruning. However, instead of relying on weight magnitude or gradient-based analysis, it directly assesses performance on a given task, making it more broadly applicable. The method is detailed in Sec. III.

### III. METHOD

#### A. Derivation

Our aim is to enable hyper-parameter tuning with gradient descent-based methods, particularly to dynamically adjust the dimensionality of neural network layers. The challenge is that dimensionality parameters are integers, whereas gradient descent requires parameters in a continuous field. We overcome this problem by adding noise to the last active element of the layer, proportional to the effect of changes in dimensionality.

Our aim is thus, for a vector  $x \in \mathbb{R}^{N \times 1}$ , to change the effective dimensionality continuously in the range  $K \in$

$[N_{\min}, N_{\max}] \in \mathbb{R}$ . For this purpose, we define a vector  $x_K \in \mathbb{R}^{N \times 1}$  as (cf. Fig. 1)

$$x_K = \left[ \underbrace{\xi_1, \xi_2, \dots, \xi_{\lfloor K \rfloor - 1}}_{\lfloor K \rfloor - 1}, \eta, \underbrace{0, \dots, 0}_{N - \lfloor K \rfloor} \right]^T \quad (1)$$

$$\eta = \sqrt{1 - \lambda} \xi_{\lfloor K \rfloor} + \sqrt{\lambda} \sigma_\xi \nu$$

$$\lambda = K - \lfloor K \rfloor,$$

where  $\lambda$  is the fractional part of the dimensionality which defines the amount of noise,  $\lfloor \cdot \rfloor$  signifies rounding downwards to an integer, and the scalars  $\xi_k, \nu$  are assumed to follow the normal distribution,  $\xi_{\lfloor K \rfloor} \sim \mathcal{N}(0, \sigma_\xi^2)$  and  $\nu \sim \mathcal{N}(0, 1)$ .

Since we have  $\lfloor K \rfloor$  active elements and  $N - \lfloor K \rfloor$  zeroes, the dimensionality is  $K$ . However, by adding noise  $\nu$  to  $\xi_{\lfloor K \rfloor}$ , we control the amount of information from the  $K$ th dimension,  $\xi_{\lfloor K \rfloor}$ , that is accessible in  $x_K$ . If  $\eta$  is noise-free,  $x_K$  is of dimensionality  $K$ , and with a very high noise level, information from only  $K - 1$  elements remains.

To assess the amount of information in  $\eta$ , we can define the linear (Wiener) estimator, optimal in the Minimum Mean Square Error (MMSE) sense, for  $\xi_{\lfloor K \rfloor}$  as [35]

$$\hat{\xi}_{\lfloor K \rfloor} := \eta \sqrt{1 - \lambda}. \quad (2)$$

The estimation error is  $\epsilon = \xi - \hat{\xi}$ , and the normalized squared error expectation will then be

$$\frac{E[(\xi - \hat{\xi})^2]}{\sigma_\xi^2} = \lambda. \quad (3)$$

Conversely, the signal-to-noise ratio is  $\lambda^{-1}$ .

In summary, through the interpolation between  $\xi_{\lfloor K \rfloor}$  and noise  $\nu$  in Eq. 1, we have a signal  $\eta$ . The best estimate  $\hat{\xi}_{\lfloor K \rfloor}$  of the desired signal  $\xi_{\lfloor K \rfloor}$  from  $\eta$ , has a normalized squared error expectation that is linear with  $\lambda$  and thus also linear with  $K$ . Eq. 1 thus defines a vector whose information content with respect to the input is a linear function of  $K$ . The *effective* dimensionality of  $x_K$  in terms of available information is therefore  $K$ . Moreover, since the interpolation is differentiable everywhere, Eq. 1 is compatible with gradient-based optimization via backpropagation.

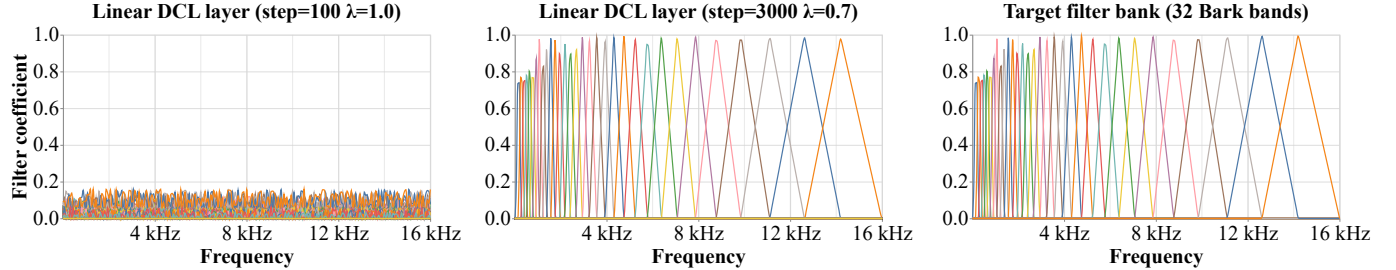


Fig. 2. Training progression of a single linear DCL to approximate a 32-band Bark filter bank. The left image shows early results after 100 steps. The middle image displays results after 3000 steps, where the estimation closely matches the target and the network's capacity is reduced by 30% ( $\lambda = 0.7$ ). The right image presents the target filter bank.

### B. Implementation details

In practice, many standard neural network layers define the size of the internal weights with a fixed dimension at instantiation time, preventing further resizing during training. In our case, we assume the initial dimensions as the maximum complexity allowed for that particular layer. We will refer to layers whose capacity remains at its maximum during the whole training procedure as *Fixed Complexity Layers* (FCL). In contrast, layers whose capacity is adjusted according to the method described in Subsec. III-A will be referred to as *Dynamic Complexity Layers* (DCL) (See Fig. 1).

Adjusting the layer capacity of DCL instances changes the output size during training. Thus, subsequent layers must adapt to these changes. To ensure compatibility, we introduce Adaptive Complexity Layers (ACL), which specify input size as a function of the preceding layer's output size rather than a fixed integer number. This approach allows these layers to remain compatible throughout the training process. It is important to note that the capacity changes in DCL instances also lead to complexity changes in ACL instances, as their input sizes adjust to maintain compatibility.

Both DCL and ACL achieve shape changes by using a subset of their weights. When the training process is completed, they can be consolidated into FCL to be used during inferences, effectively removing unused weight subsets.

## IV. CASE STUDY 1: DYNAMIC COMPLEXITY FILTER BANK

### A. Introduction

To initially validate our method, we design a simple synthetic experiment using a small network consisting of a single linear DCL. The goal of this experiment is to test the fundamental aspects of our proposed approach before extending it to more complex scenarios. This progression enables us to evaluate the core components of our method first, followed by assessing its practical utility, scalability, and robustness as shown in the next case studies detailed in Sec. V and VI.

### B. Experimental setup

In this experiment, we generate a white noise signal  $x$ , and then filter it using an unknown frequency domain filter bank  $\phi \in \{\text{bark, mel, erb}\}$ , which contains  $N \in \{16, 32, 64\}$  filters. Then, we feed the unfiltered white noise into the DCL and train

it using  $L_1$  loss, aiming to estimate the ground truth filter bank that was used to filter  $x$  as

$$\frac{1}{N} \sum_{n=0}^{N-1} |\phi(x)_n - \text{DCL}(x)_n| \quad (4)$$

This task was selected because a frequency domain filter bank can be represented using a single linear layer, thus allowing us to efficiently explore and validate our method. Additionally, because we know precisely how many parameters the model requires to accurately express the target filter bank, we can examine the extent of overparameterization reduction that our method can achieve. To quantify this, we define the overparameterization factor as

$$\text{Overparameterization factor} = \frac{\text{Network capacity}}{\text{Min. necessary capacity}} \quad (5)$$

As an example, a 32-band Bark filter bank calculated over the magnitude spectrum of a Fast Fourier Transform (FFT) of size 512 can be exactly represented as a single (257, 32) tensor. In this context, a linear DCL layer without a bias term and using a weight tensor of shape (257, 64) would be considered to have an overparameterization factor of 2, because half of its capacity is redundant for the required task. The overparameterization factor of a given architecture is usually unknown and is often minimized through informed guesses based on performance evaluations. In contrast, in our synthetic example, this factor can be accurately determined.

Following this methodology, we conducted multiple experiments by configuring the minimum complexity of the DCL to allow it to generate at least  $2N$  filters. This configuration ensures the feasibility of estimating the filter bank  $\phi$  and intentionally introduces an overparameterization by a factor of at least 2. This approach allows us to evaluate our method's effectiveness by examining the DCL's final complexity after optimizing its  $\lambda$  parameter, as previously defined in Eq. 1.

In all experiments, we trained the DCL for 3000 iterations using the Adam optimizer with a learning rate of  $1 \times 10^{-3}$ . After the first 1000 iterations, we introduce  $L_2$  regularization such that the final objective becomes

$$\frac{1}{N} \sum_{n=0}^{N-1} |\phi(x)_n - \text{DCL}(x)_n| + \frac{\beta}{N} \sum_{n=0}^{N-1} \lambda_n^2, \quad (6)$$

where  $\beta$  is the weight of the  $L_2$  regularization term. This allows the network to first move away from the random initialization, and then to simultaneously optimize both performance and complexity using our method.

### C. Results and discussion

Fig. 2 illustrates the training progression observed during the experiments: Initially, the network is randomly initialized and trained with the parameter  $\lambda$  fixed at 1.0, as shown in the left image. After 3000 steps, the predicted filter bank, displayed in the middle image, closely aligns with the target filter bank depicted in the right image. Simultaneously, the network's complexity - which was initially overparameterized - has been reduced by 30 % ( $\lambda = 0.7$ ) without a significant observable degradation in performance. We repeated the experiment using different filter banks and numbers of filters, observing comparable results.

To further explore the parameter  $\beta$ , we performed additional experiments. This time, we fixed the filter bank and, using the same setup as before, varied the value of  $\beta$  along with the overparameterization factor by using linear DCL instances of increasing sizes. The results are presented in Fig. 3. We chose to investigate overparameterization factors ranging from 2 to 10 because our experiments indicate that, with the current setup, training with higher overparameterization factors could result in noticeable degenerated filter bank shapes. Additionally, we scaled the  $L_1$  loss term by  $1 \times 10^{-3}$  to prevent its large gradients from dominating the training, given the model's small number of parameters.

It can be seen that our method effectively reduces overparameterization by up to 40 %, decreasing the factor from 10 to 6 in the most significant cases. It is also possible to observe a predominantly linear trend as the input overparameterization factor decreases. Depending on the choice of  $\beta$ , this linear behavior ceases at a certain point, resulting in no significant reduction for smaller overparameterization factors. As the value of  $\beta$  decreases, this inflection point shifts higher, indicating that - as expected - larger values of  $\beta$  enable more aggressive attempts at reducing overparameterization. However, this may potentially lead to earlier trade-offs in terms of performance.

## V. CASE STUDY 2: VOICE ACTIVITY DETECTION

### A. Introduction

Voice activity detection (VAD) refers to methods used to identify speech presence or absence in audio segments. It plays a critical role in downstream tasks such as automatic speech recognition and audio coding, optimizing processing by focusing on speech regions. Typically, VAD systems use a binary mask derived from speech presence probability (SPP) values ranging from 0.0 to 1.0 or other similar approaches, allowing systems to threshold these values to meet specific task requirements [36].

In scenarios with clean speech or a high signal-to-noise ratio (SNR), simple techniques based on energy thresholding or basic time-domain features can be effective for VAD. However, accurately detecting speech in the presence of noise or reverberation is significantly more challenging; therefore,

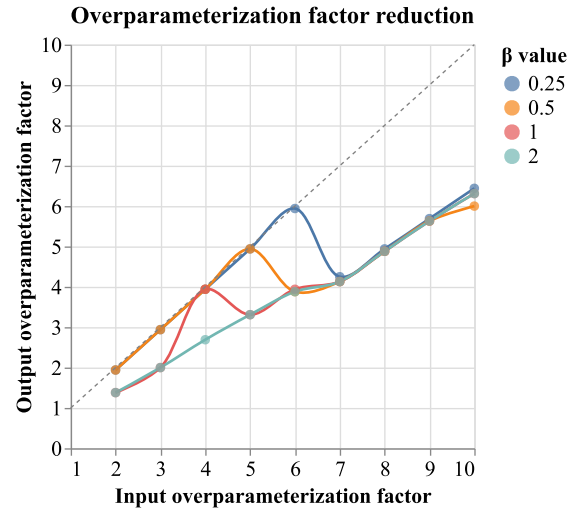


Fig. 3. Overparameterization factor reduction for different increasing values of  $\beta$ , expressed as the relationship between input overparameterization factor and output overparameterization factor. Values along the gray dashed diagonal line indicate no overparameterization reduction.

neural networks are often used due to their strong pattern recognition abilities [37]–[41].

To further test our method, we employed VAD as an example task and trained a lightweight causal neural network to predict speech presence probability in noisy and reverberant conditions.

### B. Model

Our baseline model, CRNNVAD, is a convolutional recurrent neural network that processes an 80-band log mel filter bank derived from the input waveform. It uses an FFT size of 1024 samples and a hop size of 256 samples. The output of the model is a single value per audio frame, which indicates the probability of speech presence, as illustrated in Fig.4.

The network consists of a single Conv1d layer followed by a tanh activation function, and a Gated Recurrent Unit (GRU) followed by a linear layer to combine features into a single output value. The kernel size of the input convolutional layer determines the number of lookahead frames. We used a kernel size of 3, resulting in 2 lookahead frames. The final output is passed through a sigmoid function to produce a value between 0.0 and 1.0, which can be interpreted as the SPP.

In addition to the aforementioned baseline, we implemented a dynamic complexity variant (DynCRNNVAD). In this variant, the filter bank is replaced by a DynamicLinear layer, initialized as an 80-mel filter bank, but allowing bands to be dynamically removed during optimization. Additionally, we use an AdaptiveConv1d layer, which dynamically adjusts its channels to match the output size of the DynamicLinear layer, thereby effectively reducing complexity and the number of mel bands in the filter bank.

### C. Dataset

To create our training set, we downsampled the EARS dataset [42] to 16 kHz to obtain clean speech data. Then,

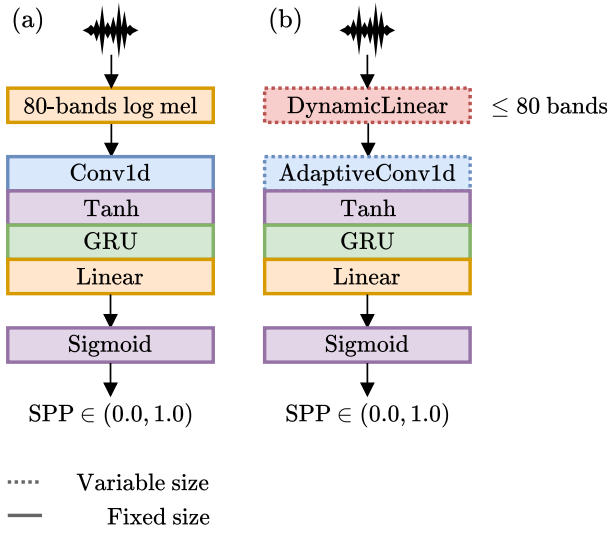


Fig. 4. Speech presence probability network. (a) represents the fixed complexity network (CRNNVAD), and (b) is the dynamic complexity variant (DynCRNNVAD). Blocks with dotted line borders can be resized during training as part of the complexity optimization process.

we convolve it with room impulse responses generated using the `pyroomacoustics` [43] package with a 25 % of probability. The reverberation time (RT60) of these room impulse responses is randomly sampled between 0 s and 1.5 s. Subsequently, the speech was mixed with noise with a 75 % probability using a randomly sampled SNR between -5 dB to 40 dB. The AudioSet partition of the DNS Challenge dataset [44] was used as our noise source. Ground truth labels are derived by applying root mean square (RMS) thresholding to the clean speech stem. This entire process occurs on-the-fly during training, with validation conducted using a separate, disjoint set from the same sources.

To test our models on unseen data, we used the VCTK dataset [45] as the speech source, a separate set of room impulse responses generated with `pyroomacoustics`, and noise sourced from the ESC-50 dataset [46] to create a fixed set of 2000 samples to compare our models.

#### D. Experiments

We first train a CRNNVAD model with fixed complexity to be used as a baseline. Then, we train multiple instances of DynCRNNVAD – the dynamic variant – starting from the same conditions as CRNNVAD, but targeting different lower limits of complexity optimization by limiting the minimum value of the  $\lambda$  parameters.

We train CRNNVAD for 200 epochs using Binary Cross Entropy Loss as the sole training objective, defined as

$$\mathcal{L}_{\text{BCE}}(y, \hat{y}) = -\frac{1}{N} \sum_{n=0}^{N-1} \left( y_n \cdot \log(\hat{y}_n) + (1 - y_n) \cdot \log(1 - \hat{y}_n) \right), \quad (7)$$

where  $y_n \in \{0, 1\}$  is the true label and  $\hat{y}_n \in (0, 1)$  is the predicted probability. For DynCRNNVAD, we train the model in two phases. First, we train the model with the complexity fixed for 100 epochs, using the same objective as CRNNVAD.

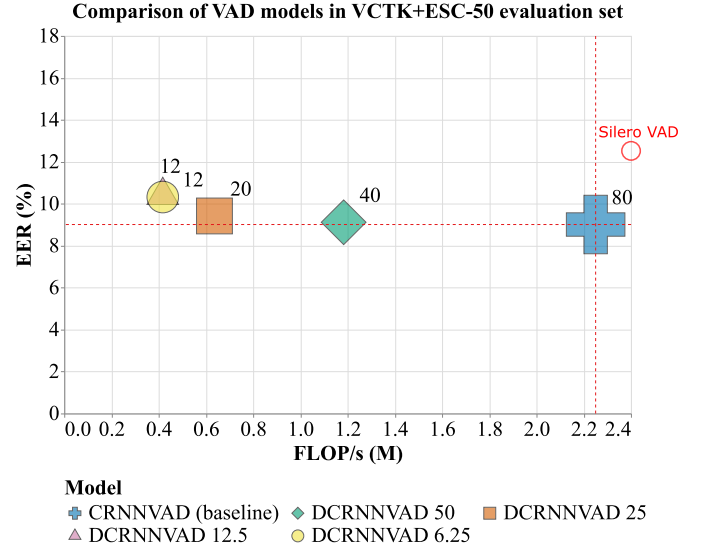


Fig. 5. Comparison between CRNNVAD baseline and the DynCRNNVAD (DCRNNVAD) models in terms of complexity, performance, and filter bank size. The x-axis shows FLOP/s, and the y-axis indicates EER on the VCTK+ESC-50 set. Numbers next to model figures denote filter bank bands. Numerical suffixes in model names denote minimum allowed complexity percentage. Silero VAD is also used as an additional benchmark, though its complexity is not reported.

Then, we train it for an additional 100 epochs, in which the complexity can be reduced by introducing  $L_2$  regularization for the  $\lambda$  term as

$$\mathcal{L}(y, \hat{y}, \lambda_0, \dots, \lambda_{N-1}) = \mathcal{L}_{\text{BCE}}(y, \hat{y}) + \frac{\beta}{N} \sum_{n=0}^{N-1} \lambda_n^2, \quad (8)$$

using  $\beta = 0.5$ . This ensures that the model begins the complexity-reduction process with well-trained weights. For all experiments, we use a batch size of 32 and an AdamW optimizer with a learning rate of  $1 \times 10^{-3}$  and a weight decay of  $1 \times 10^{-2}$ .

As an additional benchmark, we trained the popular Silero VAD [47]<sup>2</sup> using the same setup to provide a performance reference for our models.

#### E. Results and discussion

For all models, we calculated the Equal Error Rate (EER) to evaluate performance, which corresponds to the threshold  $t$  where False Positive Rate (FPR) and True Positive Rate (TPR) are equal, defined as

$$\text{EER} = \frac{\text{FAR}_t + (1 - \text{FRR}_t)}{2}, \quad t = \arg \min_t |\text{FAR}_t - \text{FRR}_t|. \quad (9)$$

FRR is the False Rejection Ratio and hence TPR = 1 - FRR. A lower EER indicates a better performing model.

Additionally, we present the number of bands in the resulting filter bank, as well as the floating-point operations per second (FLOP/s) estimated using the `moduleprofiler` package [48], as a way to characterize the performance and complexity trade-off. The results of all trained models are

<sup>2</sup>Trained using open VAD implementation: <https://github.com/stefanwebb/open-voice-activity-detection>

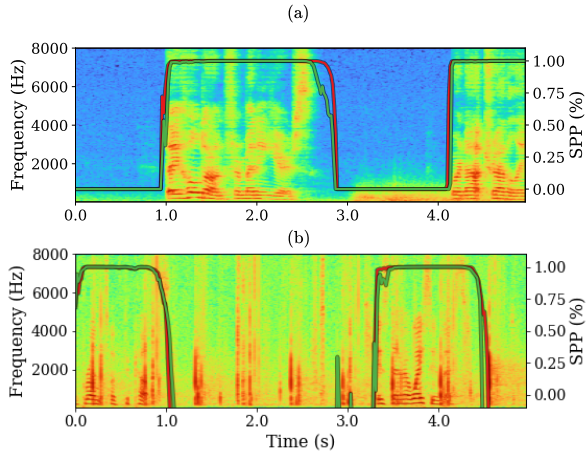


Fig. 6. Comparison between CRNNVAD baseline (red line) and DCRNNVAD 6.25 (green line) SPP predictions on (a) high SNR and (b) low SNR scenarios of VCTK+ESC-50 samples.

presented in Fig. 5. CRNNVAD is our baseline, and all DCRNNVAD models correspond to DynCRNNVAD variants. The suffixed number corresponds to the minimum possible complexity for that variant in percentage.

While our primary aim is not to achieve state-of-the-art performance in VAD but rather to evaluate the effectiveness of our method, all resulting models outperform Silero VAD. Reducing complexity by nearly 50 % has minimal impact on model performance, as observed when comparing the EER of CRNNVAD (baseline) with DCRNNVAD 50 in Fig. 5. It also halves the filter bank size, enhancing computational efficiency with negligible performance degradation. Further complexity reductions can result in slightly less performant models, such as DCRNNVAD 12.5 or DCRNNVAD 6.25, yet computational complexity can be reduced by as much as 80 %, making such models suitable for devices with very limited computational resources. It is also possible to observe that both DCRNNVAD 12.5 and DCRNNVAD 6.25 converge to a similar solution. We hypothesize that this is due to the performance-related term in the loss function dominating the optimization process. When reducing complexity results in significant performance degradation, it serves as a contention measure for degenerated models. Fig. 6 compares the SPP predictions by CRNNVAD (red line) and DCRNNVAD 6.25 (green line). The complexity-optimized model, despite having a reduced filter bank and lower complexity, can still produce SPP estimates that are highly correlated with those of the baseline model, even for unseen inputs and across different SNR levels. This demonstrates the effectiveness of our method in balancing performance and complexity during training.

## VI. CASE STUDY 3: AUDIO ANTI-SPOOFING

### A. Introduction

To further evaluate the practical utility, robustness, and scalability of our method, we apply it to the task of audio anti-spoofing. Audio anti-spoofing is the process of detecting and preventing attempts to manipulate or forge audio signals

with the intent to deceive systems, such as voice authentication or speaker verification platforms [49]. This involves analyzing the audio input to distinguish real speech signals from those that are replayed, synthesized, or otherwise tampered. Anti-spoofing efforts aim to safeguard the security and integrity of systems that rely on voice-based interactions.

Due to the increasing realism and naturalness of text-to-speech and voice conversion technologies, multiple machine learning solutions have been proposed as countermeasures (CM) to detect fake audio samples [50]–[54]. A CM is typically an audio classifier that is trained to categorize a given input signal as *bona fide* (real) or *spoof* (fake). Notable challenges such as the ASVspoof challenge have greatly contributed to advance research in this domain [55].

In our experiment, we used the datasets and evaluation plan provided by the guidelines of this challenge [56] to easily compare our results within a predefined framework. Our experimental setup is detailed in following subsections.

### B. Model

To effectively evaluate the complexity savings achieved by our method, we focus on a specific architecture. For this case study, we use the ResNet34 model [57]. It consists of four sequential stacks of residual blocks with depths 3, 4, 6, 3. Each residual block contains two sequences of layers in the order: Conv2d → BatchNorm2d → ReLU, along with a skip connection. This model was selected due to its deeper architecture and substantially larger size compared to those used in previous case studies.

To introduce our dynamic complexity method, we incorporated a DynamicLinear layer at the end of each residual block. The complexity of the model is optimized during training using our method. Each layer connected to the DynamicLinear layer is adapted to dynamically utilize a subset of its weights, thereby matching the variable output size of the DynamicLinear layer during training. We refer this model variant as DynResNet34. All model variants take an input waveform and extract the 80-bands log mel filter bank that is first processed by an initial Conv2d → BatchNorm2d → ReLU before being fed to the residual blocks. The output of the residual blocks is fed to an Attentive Statistic Pooling Layer [58] followed by a final Linear layer that computes the logits. Fig. 7 illustrates the architectures.

### C. Dataset

We used the ASVspoof 2019 LA dataset to train our models [56]. Following the ASVspoof challenge guidelines, we exclusively used the training set for model training, the development set for validating model progress, and the evaluation set to calculate the resulting metrics. The dataset includes *bona fide* utterances from 40 speakers, consisting of 16 male and 24 female speakers. *Spoof* utterances in the training and development sets were generated using 7 different voice conversion and text-to-speech algorithms, referred to as A0 through A6. The remaining algorithms, A07 to A19, were reserved for evaluating and analyzing the models' generalization capabilities. The ASVspoof 2019 LA dataset comprises

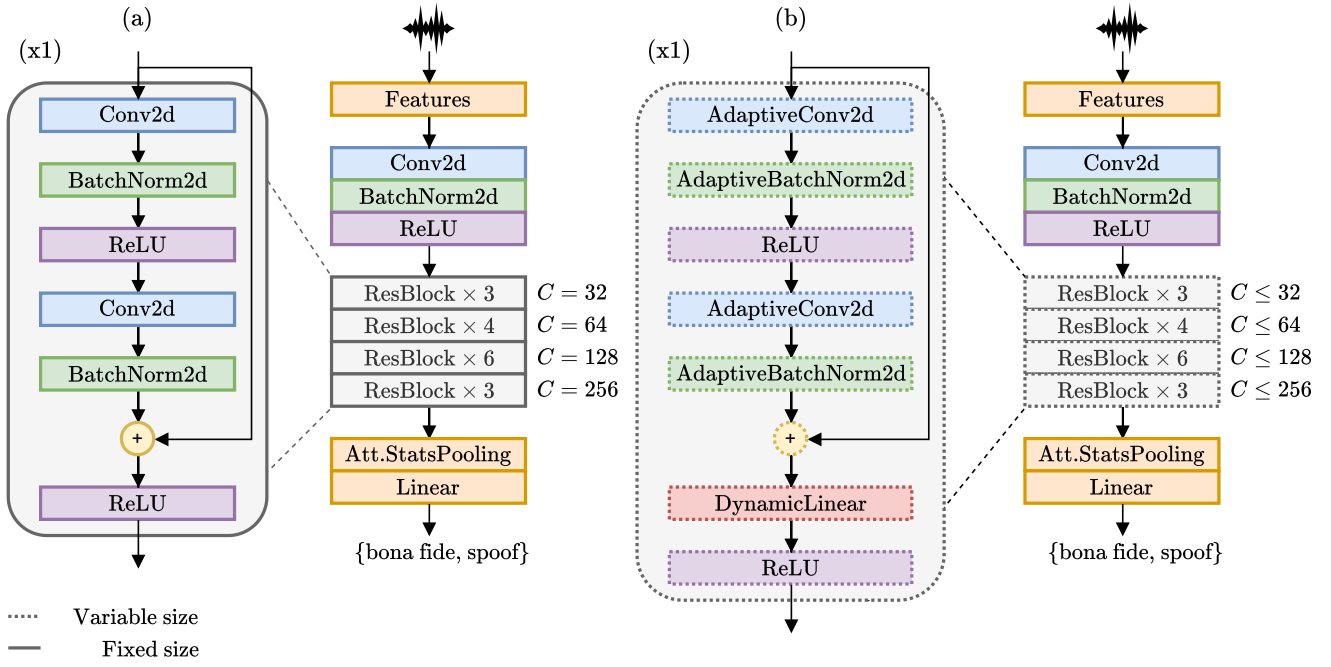


Fig. 7. Comparison between (a) Fixed complexity ResNet34, and (b) DynResNet34 (ours). Blocks with dotted line borders are resized at training time as part of the complexity optimization process. Once the training is completed, these are consolidated to a fixed size to be used during inference.  $C$  denotes the number of convolutional channels in each ResBlock, where '=' indicates fixed number of channels and ' $\leq$ ' indicates that this number may decrease during the optimization process due to dynamic complexity and adaptive layers.

approximately 111 hours of audio data, divided into 24 hours for the training set, 24 hours for the development set, and 63 hours for the evaluation set.

#### D. Experiments

As a first step, we trained a fixed complexity ResNet34 model. This model is our baseline. Subsequently, we conducted two experiments: a *single layer complexity experiment* and an *overall model complexity experiment*. For each of these experiments, we trained multiple instances of the DynResNet34 model variant.

In the *single layer complexity experiment* we allow only one of the residual block (ResBlock) stacks within the DynResNet34 model to vary its complexity, while maintaining the rest of the model fixed. This approach enables us to assess which specific block stack might hold the most important features for distinguishing between *bona fide* and *spoof* samples. Additionally, this experiment allows us to evaluate the feasibility of our method when applied to subsets of a larger model.

In the *overall complexity experiment*, we allow the DynResNet34 model to adjust the complexity of any of the residual block stacks during each step. This approach reduces computational requirements by jointly optimizing all complexity components across the model. By optimizing a larger number of parameters simultaneously, we assess the scalability of our method, evaluating its ability to maintain good performance and stable training in this setting.

In all experiments, we train the model in two phases. In the first phase, we begin by training the model with a fixed complexity for 100 epochs. We use a batch size of 32

and an AdamW optimizer configured with a learning rate of  $1 \times 10^{-3}$  and a weight decay of  $1 \times 10^{-2}$ . As in the previous case study, Binary Cross Entropy Loss is used as the sole training objective during the first phase. However, we weight the positive examples by a factor of 1.5 to compensate for the fact that they occur less frequently in the training set.

In the second phase, we train the model for an additional 100 epochs, and now include  $L_2$  regularization on the  $\lambda$  parameters of all dynamic complexity layers with  $\beta = 1.0$ .

For both *single-layer complexity experiment* and *overall complexity experiment*, we performed multiple runs that only differ in the minimum allowed complexity (i.e., minimum value allowed for  $\lambda$ ).

#### E. Results and discussion

We report performance and complexity metrics for both the *single layer complexity experiment* and the *overall complexity experiment*. For performance, we calculate the Equal Error Rate (EER), while for model complexity, we report the resulting number of model weights and the floating-point operations per seconds (FLOP/s) estimated using the moduleprofiler [48] package.

All metrics are calculated in the ASVspoof19 LA evaluation set, which comprises *spoof* samples generated by thirteen unseen algorithms during training (A07 to A19). This approach allows us to assess the generalization capabilities of our models and provides a basis for comparing their performance against the models and baselines from ASVspoof19 challenge participants.

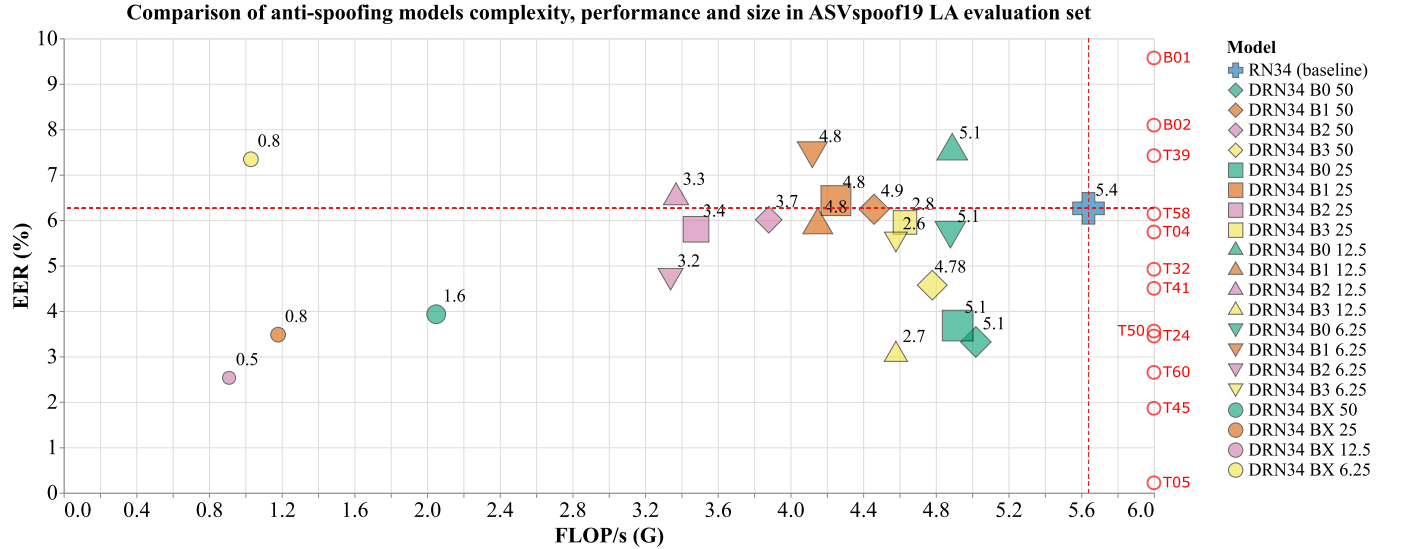


Fig. 8. Comparison of complexity, model size, and performance of DynResNet34 (DRN) models against our baseline ResNet34 (RN). The x-axis shows the complexity in FLOP/s, while the y-axis represents the Equal Error Rate on the ASVspoof19 LA evaluation set as a percentage. The number adjacent to each figure specifies the model's parameter count in millions. A number or letter following the 'B' denotes which residual block stack's complexity was optimized during training, with 'X' meaning all of them. The final number indicates the minimum complexity percentage to which the model was constrained. The top ten ASVspoof19 team submissions (with unreported complexity) and baselines, B01 and B02, appear on the secondary y-axis.

All results are shown in Fig. 8, where RN34 refers to ResNet34, our baseline model, while DRN34 denotes DynResNet34, which is optimized using our method. The numeral or letter following 'B' indicates which ResBlock stack undergoes complexity optimization. Numbers 0 to 3 correspond to individual block stacks, and 'X' means all of them. The final number specifies the minimum value of the  $\lambda$  parameters, which we constrain to study the impact of this lower limit on training dynamics. As an example, 'DRN34 BX 25' indicates a DynResNet34 model where the complexity of all block stacks is optimized, allowing reduction to a minimum of 25 % of their initial complexity. The number next to each figure indicates the model's parameter count in millions. All models were selected based on their performance on the development set. In addition, we added a secondary y-axis with the EER results of the top ten team submissions of the ASVspoof19 challenge, and the two baselines B01, and B02. Please note that the complexity metrics for these models is not reported in [59].

It is possible to observe that the majority of models not only reduce their complexity, but simultaneously decrease their EER, indicating that the redundant weights of the baseline model affect both complexity and performance. Additionally, setting the minimum value of  $\lambda$  to an extremely low value, such as 12.5 or 6.25, may degrade model performance. This trend can be observed in models positioned in the upper quadrant relative to the baseline (above the red dotted line). We hypothesize that in such cases, the  $\lambda$  parameters are optimized more aggressively compared to models with higher minimum values of  $\lambda$ , potentially resulting in different training dynamics that can hinder potential performance improvements.

In addition to this, we demonstrate that models optimized for complexity across all residual block stacks, rather than individual ones, can achieve greater improvements in both

performance and complexity. More specifically, DRN34 BX 12.5 reduces the EER from 6.26 % to 2.53 %, achieves a model size reduction of approximately 90 %, and a corresponding complexity reduction of nearly 84 %. Furthermore, in this scenario, the sequence of convolutional channels in the baseline from the first to the last ResBlock stack transitions from the original  $\{32, 64, 128, 256\}$  progression in RN34 (baseline) to  $\{5, 9, 17, 42\}$  in the optimized DRN34 BX 12.5 model. This adjustment during training allows the model to exploit emerging patterns in the data that are not easily leveraged by conventional heuristic layer size choices.

Although our primary aim is not to achieve state-of-the-art anti-spoofing performance, but rather to demonstrate the effectiveness of our method across various scenarios, the resulting DRN34 BX 12.5 model significantly outperforms the ASVspoof19 LA scenario baselines B01 and B02. Furthermore, its performance is comparable to that of top-ranked submissions, which correspond to ensemble models, whereas our approach uses a single-system model. This outcome underscores the efficacy of our method in producing a model that is not only more compact but also superior in performance to the original baseline.

## VII. CONCLUSION

We present a novel complexity reduction method for neural networks to jointly optimize complexity and performance during training. Unlike other approaches, such as model pruning, knowledge distillation, or neural architecture search, our method accomplishes this in a single training run. It neither requires a teacher model nor makes specific assumptions about the importance of different model weights.

We evaluate our approach using three speech processing case studies of increasing complexity: a synthetic audio filter bank example, a VAD model, and an audio anti-spoofing

model. The results show that our method leads to substantial complexity reduction, paired with performance outcomes ranging from marginal degradation to considerable improvements. Specifically, in the VAD case, we observed an approximately 80 % reduction in complexity, paired with a degradation in EER of less than 1.5 %. Notably, in the audio anti-spoofing case, we observed an EER improvement from 6.26 % to 2.53 % and a complexity reduction of nearly 84 %, resulting in a 90 % reduction in model size. This approach also enables the layer parameter choices to be directly learned from the data, outperforming conventional heuristic layer-size choices.

### ACKNOWLEDGMENTS

The calculations presented in this publication were carried out using the computer resources of the Aalto University of Science “Science-IT” project.

### REFERENCES

- [1] S. T. Yousif and B. M. Mahmod, “Speech enhancement algorithms: A systematic literature review,” *Algorithms*, vol. 18, no. 5, p. 272, 2025. [Online]. Available: <https://doi.org/10.3390/a18050272>
- [2] M. Li, Y. Ahmadiadi, and X.-P. Zhang, “A survey on speech deepfake detection,” *ACM Computing Surveys*, vol. 58, no. 1, pp. 1–39, 2025.
- [3] H. Kheddar, M. Hemis, and Y. Himeur, “Automatic speech recognition using advanced deep learning approaches: A survey,” *Information fusion*, vol. 109, p. 102422, 2024.
- [4] S. Braun, H. Gamper, C. K. Reddy, and I. Tashev, “Towards efficient models for real-time deep noise suppression,” in *IEEE International Conference on Acoustics, Speech and Signal Processing (ICASSP)*. IEEE, 2021, pp. 656–660. [Online]. Available: <https://doi.org/10.1109/ICASSP39728.2021.9413580>
- [5] I. Yakovlev, R. Makarov, A. Balykin, P. Malov, A. Okhotnikov, and N. Torgashov, “Reshape dimensions network for speaker recognition,” in *Interspeech 2024*. Kos, Greece: ISCA, Sep. 2024, pp. 3235–3239. [Online]. Available: <https://doi.org/10.21437/Interspeech.2024-2116>
- [6] A. E. Brownlee, J. Adair, S. O. Haraldsson, and J. Jabbo, “Exploring the accuracy – energy trade-off in machine learning,” in *2021 IEEE/ACM International Workshop on Genetic Improvement (GI)*, 2021, pp. 11–18. [Online]. Available: <https://doi.org/10.1109/GI52543.2021.00011>
- [7] N. Srivastava, G. Hinton, A. Krizhevsky, I. Sutskever, and R. Salakhutdinov, “Dropout: a simple way to prevent neural networks from overfitting,” *The journal of machine learning research*, vol. 15, no. 1, pp. 1929–1958, 2014.
- [8] C. Cortes, M. Mohri, and A. Rostamizadeh, “L2 regularization for learning kernels,” in *Proceedings of the Twenty-Fifth Conference on Uncertainty in Artificial Intelligence*, ser. UAI ’09. Arlington, Virginia, USA: AUAI Press, 2009, p. 109–116.
- [9] R. Krishnamoorthi, “Quantizing deep convolutional networks for efficient inference: A whitepaper,” *arXiv preprint arXiv:1806.08342*, vol. 2, 1806. [Online]. Available: <https://doi.org/10.48550/arXiv.1806.08342>
- [10] A. Gholami, S. Kim, Z. Dong, Z. Yao, M. W. Mahoney, and K. Keutzer, “A survey of quantization methods for efficient neural network inference,” in *Low-power computer vision*. Chapman and Hall/CRC, 2022, pp. 291–326.
- [11] G. Hinton, O. Vinyals, and J. Dean, “Distilling the knowledge in a neural network,” *arXiv preprint arXiv:1503.02531*, 2015. [Online]. Available: <https://doi.org/10.48550/arXiv.1503.02531>
- [12] J. Gou, B. Yu, S. J. Maybank, and D. Tao, “Knowledge distillation: A survey,” *International journal of computer vision*, vol. 129, no. 6, pp. 1789–1819, 2021.
- [13] S. Han, J. Pool, J. Tran, and W. Dally, “Learning both weights and connections for efficient neural network,” *Advances in neural information processing systems*, vol. 28, 2015.
- [14] S. Dave, R. Baghdadi, T. Nowatzki, S. Avancha, A. Shrivastava, and B. Li, “Hardware acceleration of sparse and irregular tensor computations of ml models: A survey and insights,” *Proceedings of the IEEE*, vol. 109, no. 10, pp. 1706–1752, 2021. [Online]. Available: <https://doi.org/10.1109/JPROC.2021.3098483>
- [15] J. O. Neill, G. V. Steeg, and A. Galstyan, “Compressing deep neural networks via layer fusion,” *arXiv preprint arXiv:2007.14917*, 2020. [Online]. Available: <https://doi.org/10.48550/arXiv.2007.14917>
- [16] J. Frankle and M. Carbin, “The lottery ticket hypothesis: Finding sparse, trainable neural networks,” in *International Conference on Learning Representations*, 2019.
- [17] Y. LeCun, J. Denker, and S. Solla, “Optimal brain damage,” *Advances in neural information processing systems*, vol. 2, 1989.
- [18] P. Molchanov, S. Tyree, T. Karras, T. Aila, and J. Kautz, “Pruning convolutional neural networks for resource efficient inference,” in *International Conference on Learning Representations (ICLR)*, 2017.
- [19] M. Zhu and S. Gupta, “To prune, or not to prune: exploring the efficacy of pruning for model compression,” *International Conference on Learning Representations (ICLR)*, 2017.
- [20] T. Gale, E. Elsen, and S. Hooker, “The state of sparsity in deep neural networks,” *arXiv preprint cs.LG/1902.09574*, 2019. [Online]. Available: <https://doi.org/10.48550/arXiv.1902.09574>
- [21] T. Lin, S. U. Stich, L. Barba, D. Dmitriev, and M. Jaggi, “Dynamic model pruning with feedback,” *International Conference on Learning Representations (ICLR)*, 2020.
- [22] Y. Chen, Z. Ma, W. Fang, X. Zheng, Z. Yu, and Y. Tian, “A unified framework for soft threshold pruning,” *International Conference on Learning Representations (ICLR)*, 2023.
- [23] Y. Liu, H. Xiong, J. Zhang, Z. He, H. Wu, H. Wang, and C. Zong, “End-to-end speech translation with knowledge distillation,” in *Interspeech*, 2019, pp. 1128–1132. [Online]. Available: <https://doi.org/10.21437/Interspeech.2019-2582>
- [24] S. Gandhi, P. Von Platen, and A. M. Rush, “Distil-whisper: Robust knowledge distillation via large-scale pseudo labelling,” *arXiv preprint arXiv:2311.00430*, 2023. [Online]. Available: <https://doi.org/10.48550/arXiv.2311.00430>
- [25] J. Xue, C. Fan, J. Yi, C. Wang, Z. Wen, D. Zhang, and Z. Lv, “Learning from yourself: A self-distillation method for fake speech detection,” in *IEEE International Conference on Acoustics, Speech and Signal Processing (ICASSP)*, 2023, pp. 1–5. [Online]. Available: <https://doi.org/10.1109/ICASSP49357.2023.10096837>
- [26] G. Woo Lee, H. Kook Kim, and D.-J. Kong, “Knowledge distillation-based training of speech enhancement for noise-robust automatic speech recognition,” *IEEE Access*, vol. 12, pp. 72 707–72 720, 2024. [Online]. Available: <https://doi.org/10.1109/ACCESS.2024.3403761>
- [27] C. White, M. Safari, R. Sukthanker, B. Ru, T. Elsken, A. Zela, D. Dey, and F. Hutter, “Neural architecture search: Insights from 1000 papers,” *arXiv preprint arXiv:2301.08727*, 2023. [Online]. Available: <https://doi.org/10.48550/arXiv.2301.08727>
- [28] R. Luo, X. Tan, R. Wang, T. Qin, J. Li, S. Zhao, E. Chen, and T.-Y. Liu, “Lightspeech: Lightweight and fast text to speech with neural architecture search,” in *IEEE International Conference on Acoustics, Speech and Signal Processing (ICASSP)*, 2021, pp. 5699–5703. [Online]. Available: <https://doi.org/10.1109/ICASSP39728.2021.9414403>
- [29] Y. Liu, T. Li, P. Zhang, and Y. Yan, “Nas-scae: Searching compact attention-based encoders for end-to-end automatic speech recognition,” in *Interspeech*, 2022, pp. 1011–1015. [Online]. Available: <https://doi.org/10.21437/Interspeech.2022-748>
- [30] J.-H. Lee, J.-H. Chang, J.-M. Yang, and H.-G. Moon, “Nas-tasnet: Neural architecture search for time-domain speech separation,” *IEEE Access*, vol. 10, pp. 56 031–56 043, 2022. [Online]. Available: <https://doi.org/10.1109/ACCESS.2022.3176003>
- [31] C. Ying, A. Klein, E. Christiansen, E. Real, K. Murphy, and F. Hutter, “Nas-bench-101: Towards reproducible neural architecture search,” in *International conference on machine learning*. PMLR, 2019, pp. 7105–7114.
- [32] Y. Han, G. Huang, S. Song, L. Yang, H. Wang, and Y. Wang, “Dynamic neural networks: A survey,” *IEEE transactions on pattern analysis and machine intelligence*, vol. 44, no. 11, pp. 7436–7456, 2021. [Online]. Available: <https://doi.ieeecomputersociety.org/10.1109/TPAMI.2021.3117837>
- [33] R. Miccini, A. Zniber, C. Laroche, T. Piechowiak, M. Schoeberl, L. Pezzarossa, O. Karrakchou, J. Sparsø, and M. Ghogho, “Dynamic nsnet2: Efficient deep noise suppression with early exiting,” in *2023 IEEE 33rd International Workshop on Machine Learning for Signal Processing (MLSP)*. IEEE, 2023, pp. 1–6. [Online]. Available: <https://doi.org/10.1109/MLSP55844.2023.10285925>
- [34] R. Miccini, M. Kim, C. Laroche, L. Pezzarossa, and P. Smaragdis, “Adaptive slimming for scalable and efficient speech enhancement,” *IEEE Workshop on Applications of Signal Processing to Audio and Acoustics (WASPAA)*, 2025. [Online]. Available: <https://doi.org/10.1109/WASPAA66052.2025.11230950>

[35] A. V. Oppenheim, A. S. Willsky, and S. H. Nawab, *Signals & systems*. Pearson Educación, 1997.

[36] T. Bäckström, O. Räsänen, A. Zewoudie, P. P. Zarazaga, L. Koivusalo, S. Das, E. G. Mellado, M. B. Mansali, D. Ramos, S. Kadiri, P. Alku, and M. H. Vali, *Introduction to Speech Processing*, 2nd ed., 2022. [Online]. Available: <https://speechprocessingbook.aalto.fi>

[37] T. Hughes and K. Mierle, "Recurrent neural networks for voice activity detection," in *2013 IEEE International Conference on Acoustics, Speech and Signal Processing*, 2013, pp. 7378–7382. [Online]. Available: <https://doi.org/10.1109/ICASSP.2013.6639096>

[38] A. Sehgal and N. Kehtarnavaz, "A convolutional neural network smartphone app for real-time voice activity detection," *IEEE Access*, vol. 6, pp. 9017–9026, 2018. [Online]. Available: <https://doi.org/10.1109/ACCESS.2018.2800728>

[39] F. Eyben, F. Weninger, S. Squartini, and B. Schuller, "Real-life voice activity detection with lstm recurrent neural networks and an application to hollywood movies," in *2013 IEEE International Conference on Acoustics, Speech and Signal Processing*, 2013, pp. 483–487. [Online]. Available: <https://doi.org/10.1109/ICASSP.2013.6637694>

[40] S. Mihalache, I.-A. Ivanov, and D. Burileanu, "Deep neural networks for voice activity detection," in *2021 44th International Conference on Telecommunications and Signal Processing (TSP)*, 2021, pp. 191–194. [Online]. Available: <https://doi.org/10.1109/TSP52935.2021.9522670>

[41] H. Dinkel, S. Wang, X. Xu, M. Wu, and K. Yu, "Voice activity detection in the wild: A data-driven approach using teacher-student training," *IEEE/ACM Transactions on Audio, Speech, and Language Processing*, vol. 29, pp. 1542–1555, 2021. [Online]. Available: <https://doi.org/10.1109/TASLP.2021.3073596>

[42] J. Richter, Y.-C. Wu, S. Krenn, S. Welker, B. Lay, S. Watanabe, A. Richard, and T. Gerkmann, "EARS: An anechoic fullband speech dataset benchmarked for speech enhancement and dereverberation" in *ISCA Interspeech*, 2024, pp. 4873–4877. [Online]. Available: <https://doi.org/10.21437/Interspeech.2024-153>

[43] R. Scheibler, E. Bezzam, and I. Dokmanić, "Pyroomacoustics: A python package for audio room simulation and array processing algorithms," in *IEEE International Conference on Acoustics, Speech and Signal Processing (ICASSP)*, 2018, pp. 351–355. [Online]. Available: <https://doi.org/10.1109/ICASSP.2018.8461310>

[44] C. K. Reddy, H. Dubey, V. Gopal, R. Cutler, S. Braun, H. Gamper, R. Aichner, and S. Srinivasan, "ICASSP 2021 Deep Noise Suppression Challenge," in *ICASSP*, 2021. [Online]. Available: <https://doi.org/10.1109/ICASSP39728.2021.9415105>

[45] J. Yamagishi, C. Veaux, and K. MacDonald, "CSTR VCTK corpus: English multi-speaker corpus for CSTR voice cloning toolkit (version 0.92)," *Edinburgh DataShare*. [Online]. Available: <https://datashare.ed.ac.uk/handle/10283/3443>

[46] K. J. Piczak, "ESC: Dataset for Environmental Sound Classification," in *Proceedings of the 23rd Annual ACM Conference on Multimedia*. ACM Press, pp. 1015–1018. [Online]. Available: <http://dl.acm.org/citation.cfm?doid=2733373.2806390>

[47] S. Team, "Silero VAD: pre-trained enterprise-grade voice activity detector (VAD), number detector and language classifier," <https://github.com/snakers4/silero-vad>, 2024.

[48] E. Gómez, "moduleprofiler," 2024. [Online]. Available: <https://github.com/eagomez2/moduleprofiler>

[49] M. Li, Y. Ahmadadi, and X.-P. Zhang, "Audio anti-spoofing detection: A survey," *arXiv preprint arXiv:2404.13914*, 2024.

[50] Y. Ma, Z. Ren, and S. Xu, "Rw-resnet: A novel speech anti-spoofing model using raw waveform," in *Interspeech*, 2021, pp. 4144–4148. [Online]. Available: <https://doi.org/10.21437/Interspeech.2021-438>

[51] H. Tak, J. Patino, M. Todisco, A. Nautsch, N. Evans, and A. Larcher, "End-to-end anti-spoofing with rawnet2," in *IEEE International Conference on Acoustics, Speech and Signal Processing (ICASSP)*, 2021, pp. 6369–6373. [Online]. Available: <https://doi.org/10.1109/ICASSP39728.2021.9414234>

[52] J.-w. Jung, H.-S. Heo, H. Tak, H.-j. Shim, J. S. Chung, B.-J. Lee, H.-J. Yu, and N. Evans, "AASIST: Audio anti-spoofing using integrated spectro-temporal graph attention networks," in *IEEE International Conference on Acoustics, Speech and Signal Processing (ICASSP)*, 2022, pp. 6367–6371. [Online]. Available: <https://doi.org/10.1109/ICASSP43922.2022.9747766>

[53] J. Zhang, G. Tu, S. Liu, and Z. Cai, "Audio anti-spoofing based on audio feature fusion," *Algorithms*, vol. 16, no. 7, p. 317, 2023. [Online]. Available: <https://doi.org/10.3390/a16070317>

[54] A. Khan, K. M. Malik, and S. Nawaz, "Frame-to-utterance convergence: A spectra-temporal approach for unified spoofing detection," in *IEEE International Conference on Acoustics, Speech and Signal Processing* (ICASSP), IEEE, 2024, pp. 10761–10765. [Online]. Available: <https://doi.org/10.1109/ICASSP48485.2024.10447500>

[55] X. Wang, H. Delgado, H. Tak, J.-w. Jung, H.-j. Shim, M. Todisco, I. Kukanov, X. Liu, M. Sahidullah, T. Kinnunen *et al.*, "ASVspoof 5: Crowdsourced speech data, deepfakes, and adversarial attacks at scale," in *The Automatic Speaker Verification Spoofing Countermeasures Workshop (ASVspoof 2024)*, 2024, pp. 1–8. [Online]. Available: <https://doi.org/10.21437/ASVspoof.2024-1>

[56] J. Yamagishi, M. Todisco, M. Sahidullah, H. Delgado, X. Wang, N. Evans, T. Kinnunen, K. A. Lee, V. Vestman, and A. Nautsch, "ASVspoof 2019: Automatic speaker verification spoofing and countermeasures challenge evaluation plan," *ASV Spoof*, vol. 13, 2019.

[57] K. He, X. Zhang, S. Ren, and J. Sun, "Deep residual learning for image recognition," in *Proceedings of the IEEE Conference on Computer Vision and Pattern Recognition (CVPR)*, June 2016. [Online]. Available: <https://doi.org/10.1109/CVPR.2016.90>

[58] K. Okabe, T. Koshinaka, and K. Shinoda, "Attentive statistics pooling for deep speaker embedding," *Interspeech*, 2018.

[59] M. Todisco, X. Wang, V. Vestman, M. Sahidullah, H. Delgado, A. Nautsch, J. Yamagishi, N. Evans, T. Kinnunen, and K. A. Lee, "ASVspoof 2019: Future horizons in spoofed and fake audio detection," *Interspeech*, 2019.



**Esteban Gómez** received his bachelor's degree from Universidad de Chile in 2015, a master's degree from Berklee College of Music in 2017, and a second master's degree from Universitat Pompeu Fabra in 2021. He is currently pursuing a Ph.D. degree with the Department of Information and Communications Engineering at Aalto University, Finland. He has contributed to the research and development of low-complexity, real-time speech enhancement systems in collaboration with several companies. His research interests include antispoofing systems and real-time speech enhancement, with a focus on low-complexity systems.



**Tom Bäckström** (Senior member, IEEE) received the master's and Ph.D. degrees from Aalto University, Finland, in 2001 and 2004, respectively, when it was known as the Helsinki University of Technology. He was a Professor at the International Audio Laboratory Erlangen, Friedrich-Alexander University, from 2013 to 2016, and a Researcher at Fraunhofer ISS, from 2008 to 2013. Since 2016, he has been an Associate Professor with the Department of Information and Communications Engineering at Aalto University. He has contributed to several international speech and audio coding standards and is the Chair and Co-Founder of the ISCA Special Interest Group on "Security and Privacy in Speech Communication." He is the president of ISCA (2025-2027). His research interests include technologies for spoken interaction, with an emphasis on efficiency and privacy, particularly in multi-device and multi-user environments.